



Quiet High Speed Fan (QHsF) Flutter Calculations Using the TURBO Code

*Milind A. Bakhle, Rakesh Srivastava, and Theo G. Keith, Jr.
University of Toledo, Toledo, Ohio*

*James B. Min and Oral Mehmed
Glenn Research Center, Cleveland, Ohio*

NASA STI Program . . . in Profile

Since its founding, NASA has been dedicated to the advancement of aeronautics and space science. The NASA Scientific and Technical Information (STI) program plays a key part in helping NASA maintain this important role.

The NASA STI Program operates under the auspices of the Agency Chief Information Officer. It collects, organizes, provides for archiving, and disseminates NASA's STI. The NASA STI program provides access to the NASA Aeronautics and Space Database and its public interface, the NASA Technical Reports Server, thus providing one of the largest collections of aeronautical and space science STI in the world. Results are published in both non-NASA channels and by NASA in the NASA STI Report Series, which includes the following report types:

- **TECHNICAL PUBLICATION.** Reports of completed research or a major significant phase of research that present the results of NASA programs and include extensive data or theoretical analysis. Includes compilations of significant scientific and technical data and information deemed to be of continuing reference value. NASA counterpart of peer-reviewed formal professional papers but has less stringent limitations on manuscript length and extent of graphic presentations.
- **TECHNICAL MEMORANDUM.** Scientific and technical findings that are preliminary or of specialized interest, e.g., quick release reports, working papers, and bibliographies that contain minimal annotation. Does not contain extensive analysis.
- **CONTRACTOR REPORT.** Scientific and technical findings by NASA-sponsored contractors and grantees.

- **CONFERENCE PUBLICATION.** Collected papers from scientific and technical conferences, symposia, seminars, or other meetings sponsored or cosponsored by NASA.
- **SPECIAL PUBLICATION.** Scientific, technical, or historical information from NASA programs, projects, and missions, often concerned with subjects having substantial public interest.
- **TECHNICAL TRANSLATION.** English-language translations of foreign scientific and technical material pertinent to NASA's mission.

Specialized services also include creating custom thesauri, building customized databases, organizing and publishing research results.

For more information about the NASA STI program, see the following:

- Access the NASA STI program home page at <http://www.sti.nasa.gov>
- E-mail your question via the Internet to help@sti.nasa.gov
- Fax your question to the NASA STI Help Desk at 301-621-0134
- Telephone the NASA STI Help Desk at 301-621-0390
- Write to:
NASA STI Help Desk
NASA Center for AeroSpace Information
7121 Standard Drive
Hanover, MD 21076-1320



Quiet High Speed Fan (QHSF) Flutter Calculations Using the TURBO Code

*Milind A. Bakhle, Rakesh Srivastava, and Theo G. Keith, Jr.
University of Toledo, Toledo, Ohio*

*James B. Min and Oral Mehmed
Glenn Research Center, Cleveland, Ohio*

National Aeronautics and
Space Administration

Glenn Research Center
Cleveland, Ohio 44135

Acknowledgments

The authors would like to thank Dr. Josef Panovsky, Honeywell Engines & Systems, for providing the TURBO grid used in this work and for providing comments and discussions regarding the calculations. We would also like to thank Dr. Jen-Ping Chen, Mississippi State University, for providing assistance with the TURBO code, and Mr. E. Brian Fite, NASA Glenn Research Center, for making the experimental data available and for providing comments and discussions on the results. This report was originally published internally as QAT-001 in September 2002.

Level of Review: This material has been technically reviewed by technical management.

Available from

NASA Center for Aerospace Information
7121 Standard Drive
Hanover, MD 21076-1320

National Technical Information Service
5285 Port Royal Road
Springfield, VA 22161

Available electronically at <http://gltrs.grc.nasa.gov>

Quiet High Speed Fan (QHSF) Flutter Calculations Using the TURBO Code

Milind A. Bakhle, Rakesh Srivastava, and Theo G. Keith, Jr.
University of Toledo
Toledo, Ohio 43606

James B. Min and Oral Mehmed
National Aeronautics and Space Administration
Glenn Research Center
Cleveland, Ohio 44135

Introduction

A scale model of the NASA/Honeywell Engines Quiet High Speed Fan (QHSF) was tested for operability and performance. During the testing of this 18-in. scale model at the Honeywell Engines component test facility in Phoenix, Arizona in 1999, flutter was observed over a range of operating conditions. A 22-in. scale model (shown in fig. 1) was tested in 2000 at the NASA Glenn Research Center 9-by-15 Low Speed Wind Tunnel. Flutter was again observed during testing. This report documents the aeroelastic calculations done for the 22-in. QHSF scale model using the TURBO code.

TURBO Code

The TURBO code version 4.2 with aeroelastic modifications was used in all the calculations. The aeroelastic modifications allow (1) the use of steady TURBO solutions as initial guess for TURBO flutter runs, (2) the use of grid deformations in Cartesian coordinates instead of cylindrical coordinates, and (3) the calculation of aeroelastic work. The AE-prep preprocessor was used to interpolate the modal deflections from the ANSYS grid to the CFD grid, propagate the grid deformations from the blade surfaces to the interior grid points, and to generate the grid displacement data in the form required by the TURBO code. TURBO uses prescribed harmonic blade vibrations to generate the unsteady flowfield. The unsteady aerodynamic force distribution on the blade surfaces (including pressure and viscous contributions) is integrated with the blade deformations to generate a work-per-cycle. This work done on the blade during a cycle of blade vibration is then converted to an aerodynamic damping to determine flutter stability.

Steady Calculations

Steady TURBO calculations were done using a 107 by 51 by 39 (axial by radial by tangential) mesh with 45 chordwise points and 47 spanwise points on each blade surface. Steady calculations were done at rotational speeds of 15,444, 13,900, and 12,355 rpm (100, 90, and 80 percent of design speed). The prescribed back pressure values are listed in table I. The resulting operational characteristics are shown in figure 2(a) (pressure ratio vs. mass flow rate) and figure 2(b) (efficiency vs. mass flow rate). In both these figures, the calculated mass flow rate is scaled to the equivalent 18-in. scale model and reported in lbm/s units—for easy comparison with predicted and measured characteristics from (ref. 1).

TABLE I.—OPERATING CONDITIONS FOR STEADY TURBO RUNS

Speed	rpm	Back pressure (psi)
100 percent	15,444	14.7, 15.5, 16.0, 16.5, 17.0
90 percent	13,900	13.8, 14.5, 15.2, 15.6, 15.7, 15.9, 16.2, 16.4
80 percent	12,355	12.4, 13.2, 14.0, 14.8, 15.2, 15.6, 15.7

The variation of pressure ratio with mass flow rate, as calculated using the TURBO code (fig. 2(a)), is similar in trend to the measurements and to the predictions from the DAWES code (ref. 1). Differences in the levels are seen at all three speeds. The TURBO results are seen to over-predict the pressure rise at the 80 and 90 percent speeds. The DAWES results, on the other hand, are seen to under-predict the pressure rise at all three speeds. The reasons for these differences between the measured and calculated values are not understood at present. The efficiency calculated from the TURBO and DAWES codes (fig. 2(b)) is very similar in trend, with a peak seen for each speed. The peak efficiency calculated using the TURBO code is higher by two points, as compared to the DAWES results, for the 80 and 90 percent speeds. At 100 percent speed, the two codes predict nearly the same variation in efficiency, but the TURBO results are shifted towards higher mass flow rate. The measurements show that both codes under-predict the peak efficiency, and the measurements at the 80 percent speed do not include the part of the characteristic where the efficiency increases with decreasing mass flow rate.

The possible reasons for differences between the TURBO and DAWES results include differences in grid, algorithms, and turbulence model. The possible reasons for the differences between the TURBO results and measurements include: (1) the blade shape used in all the TURBO calculations was calculated using the centrifugal and aerodynamic loads at the design speed, (2) all the TURBO calculations were performed with uniform total conditions prescribed at inlet boundary, and the exit static pressure prescribed at the hub and calculated at other spanwise locations using radial equilibrium condition, and (3) a uniform tip-gap (uniform from leading edge to trailing edge) is used in all TURBO calculations.

Aeroelastic Calculations—Effect of Numerical Parameters

Aeroelastic calculations were done with the blade vibration capability of the TURBO code. The grid used was the same as that used for the steady calculations. All aeroelastic calculations were done for the 1st vibration mode at a frequency of 350.9 Hz. The mode shape was for a single blade held at the root and was calculated at the design speed. The relevant numerical parameters listed in table II were varied to establish appropriate values for all remaining calculations and to provide an estimate of the variability in the results due to numerical parameters. This numerical study was done for 100 percent speed with a back pressure of 16 psi, and a phase angle of 32.7°. In all cases, the calculations were done for 16 cycles of blade vibration using time-shift boundary conditions with a relaxation factor of 0.8.

TABLE II.—SUMMARY OF NUMERICAL PARAMETERS FOR AEROELASTIC CALCULATIONS

	Parameter	Values
1.	Blade vibration amplitude	4×10^{-5} , 2×10^{-4} , 1×10^{-3}
2.	Number of time steps per vibration cycle	100, 200, 300
3.	Max. number of Newton sub-iterations at each time step	3, 6

Blade Vibration Amplitude

The convergence to periodicity of the unsteady TURBO solutions is shown in figure 3(a) for the three amplitudes listed previously in table II. The amplitude of vibration was increased and decreased by a factor of 5 from the base value of 2×10^{-4} . The variation of aerodynamic damping with vibration amplitude

is shown in figure 3(b). The aerodynamic damping is seen to be independent of the vibration amplitude in the range of values investigated, implying a linear variation of the unsteady aerodynamics with blade vibration amplitude. The base amplitude of vibration (2×10^{-4}) was used for subsequent calculations, with exceptions as noted later.

Number of Time Steps per Vibration Cycle

The convergence to periodicity of the unsteady TURBO solutions is shown in figure 4(a) for three different time steps. Since the frequency of blade vibration is held fixed, the time step size varies inversely with the number of time steps per cycle. The number of time steps per cycle was decreased and increased by 100 from the base value of 200, as listed in table II. The resulting non-dimensional time steps were 1.7×10^{-2} , 8.7×10^{-3} , and 5.8×10^{-3} with corresponding maximum CFL numbers of 516, 258, and 172. Note that the CFL number is the time step multiplied by the local sonic velocity divided by the local grid spacing. The variation of aerodynamic damping with number of time steps per cycle is shown in figure 4(b). The aerodynamic damping is seen to be nearly the same for the 200 and 300 time steps per cycle and slightly different for 100 time steps per cycle. In order to keep computational time requirements at a reasonable level, 100 time steps per cycle were used in all subsequent calculations. However, the variability in the results due to the selected time step was noted in the evaluation of the results.

Maximum Number of Newton Sub-Iterations

The convergence to periodicity of the unsteady TURBO solutions is shown in figure 5(a) for 3 and 6 maximum Newton sub-iterations during each time step. The variation of aerodynamic damping with maximum number of Newton sub-iterations is shown in figure 5(b). The aerodynamic damping values show a small dependence on the Newton sub-iterations. The effect of going from 3 to 6 maximum Newton sub-iterations is similar to the effect of increasing the number of time steps per cycle from 100 to 200. Also, in both cases, the computational time requirements are nearly doubled. In order to keep computational time requirements at a reasonable level, 3 maximum Newton sub-iterations were used in all subsequent calculations. The variability in the results due to the maximum number of Newton sub-iterations was noted in the evaluation of the results.

As a result of the numerical study, it was established that the variability or possible error in the aerodynamic damping was approximately 0.1 percent for the base case. This variability was related to the time step and the maximum number of Newton sub-iterations. With more computational resources available, it would be recommended that calculations be done with 200 time steps per cycle and 6 maximum Newton sub-iterations. Another source of variability in the aerodynamic damping is the grid spacing. However, the effect of grid spacing has not been investigated.

Aeroelastic Calculations at 100 Percent Speed— Effect of Interblade Phase Angle

Aeroelastic calculations were done at 8 (out of a possible 22) values of phase angles. These calculations were done for 100 percent speed with a back pressure of 16 psi. For all values of phase angle except 0° , calculations were done for 16 cycles of blade vibration using time-shift boundary conditions with a relaxation factor of 0.8. For 0° phase angle, periodic boundary conditions were used and the calculations were stopped after 8 cycles, which resulted in periodic solutions. The convergence to periodicity of the unsteady TURBO solutions is shown in figure 6(a) for the various phase angles. The variation of aerodynamic damping with phase angle is shown in figure 6(b). The range in variation of the aerodynamic damping is significantly larger than the possible error due to a choice of time step and maximum number of Newton sub-iterations. The phase angles near 0° are seen to result in the lowest values of aerodynamic damping.

Aeroelastic Calculations at 90 Percent Speed, 0° Phase Angle— Effect of Back Pressure

Aeroelastic calculations were performed for 90 percent speed at 6 of the 8 values of back pressure listed in table I, for 0° inter-blade phase angle. As before, calculations were done for 8 cycles with periodic boundary conditions. The convergence to periodicity of the unsteady TURBO solutions is shown in figure 7(a) for various back pressures. For calculations with a back pressure value of 15.9 psi, the amplitude of blade vibration was 1×10^{-3} rather than the base value of 2×10^{-4} used with all other back pressure values. The reason for this difference was that the solution for 15.9 psi back pressure with no blade vibration had an oscillatory component. Thus, the blade vibration amplitude was increased to ensure that the effects of blade vibration could be distinguished from the flow unsteadiness from other sources. The variation of aerodynamic damping with back pressure is shown in figure 7(b). For the 0° phase angle, the aerodynamic damping is seen to increase with back pressure, and then drop sharply near the stall line.

Aeroelastic Calculations at 90 Percent Speed— Effect of Interblade Phase Angle

Aeroelastic calculations were done for 90 percent speed, and back pressure values of 15.7, 15.9, and 16.4 psi. Selected phase angles near 0° were analyzed. The convergence to periodicity of the unsteady TURBO solutions is shown in figure 8(a) to (c) for back pressure values of 15.7, 15.9, and 16.4 psi, respectively. The variation of aerodynamic damping with phase angle is shown in figure 8(d). The phase angle of 0° is seen to result in the lowest values of aerodynamic damping for back pressure values of 15.7 and 15.9 psi. But, for a back pressure value of 16.4 psi, the lowest values of aerodynamic damping are seen to occur at 32.7° phase angle. In figure 8(d), the results of two other calculations are shown. These calculations were both done using 200 time steps per vibration cycle, in contrast to the 100 time steps per cycle used in all other calculations. In one of these calculations, the vibration frequency value of 315.9 Hz was used as opposed to 350.9 Hz used in all other calculations. The smaller value corresponds to the calculated blade natural frequency for 90 percent speed, whereas the larger value is that for 100 percent speed.

Aeroelastic Calculations at 90 Percent Speed, 32.7° Phase Angle— Effect of Back Pressure

Aeroelastic calculations were done for 90 percent speed at 7 of the 8 values of back pressure listed in table I, for 32.7° phase angle. Calculations were done for 16 cycles with time-shift boundary conditions. The variation of aerodynamic damping with back pressure is shown in figure 9. For the 32.7° phase angle, with increasing back pressure, the aerodynamic damping is seen to increase gradually and then drop off sharply, indicating that at 32.7° phase angle points near the stall line are less stable. The distribution of work-per-cycle on the blade surfaces is shown in figure 10 for 90 percent speed, 16.4 psi back pressure, and 32.7° phase angle. The only significant unstable region is located on the outboard portion of the suction surface in the vicinity of the shock. The leading edge region on the pressure surface near the tip of the forward-swept blade is a stable region.

Summary and Concluding Remarks

Aeroelastic calculations were done for the Quiet High Speed Fan (QHSF) using the blade vibration capability of the TURBO code. Calculations were done at 100 percent speed to quantify the effect of numerical parameters on the aerodynamic damping predictions. Blade vibration amplitude, number of

time steps per cycle (time step), and maximum number of Newton sub-iterations at each time step were varied independently. This numerical study allowed the selection of appropriate values of these parameters, and also allowed an assessment of the variability in the calculated aerodynamic damping. Each of the three parameters was seen to introduce no more than 0.1 percent variation in the aerodynamic damping (percent critical damping).

Calculations were also done at 90 percent of design speed. The predicted trends in aerodynamic damping correspond to those observed during testing. During testing, flutter was observed near the stall line at part-speed conditions; the flutter was in the first natural mode with a 2 nodal diameter forward travelling wave. The TURBO calculations at 90 percent speed showed that for the first mode, near the stall line, the phase angle with the lowest aerodynamic damping was 32.7° which corresponds to a 2 nodal diameter forward travelling wave. At this value of phase angle, the TURBO calculations showed a sharp decrease in aerodynamic damping as the back pressure was increased to approach the stall line. However, the TURBO code did not calculate negative aerodynamic damping at any of the conditions for which calculations were done. The lowest value of aerodynamic damping calculated was 0.12 percent.

The following calculations may lead to an improved understanding of the variability in the results obtained from the TURBO code: (1) calculations using a finer grid rather than the current grid which has 45 chordwise points and 47 spanwise points on each blade surface, (2) calculations using the actual blade shape at part-speed conditions rather than the blade shape from the design speed, (3) calculations using an inlet profile as opposed to the uniform total conditions currently prescribed, (4) calculations using the actual tip-gap (non-uniform from leading edge to trailing edge) rather than the constant gap currently used, (5) calculations using the mode shape for part-speed rather than that from the design speed, (6) calculations using mode shapes from cyclic symmetry calculations on the blade-disk system rather than blade-alone mode shapes.

References

1. Weir, D., "Design and Test of Fan/Nacelle Models, Quiet High-Speed Fan," NASA Contractor Report, NASA/CR—2003-21237 April 2003.



Figure 1.—22-in. scale model of Quiet High Speed Fan (QHSF).

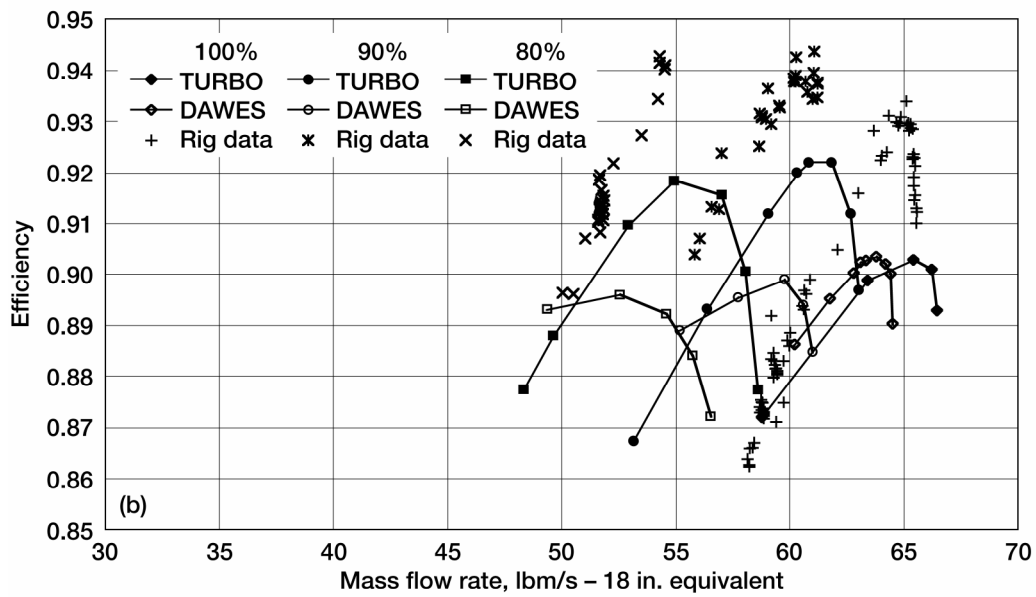
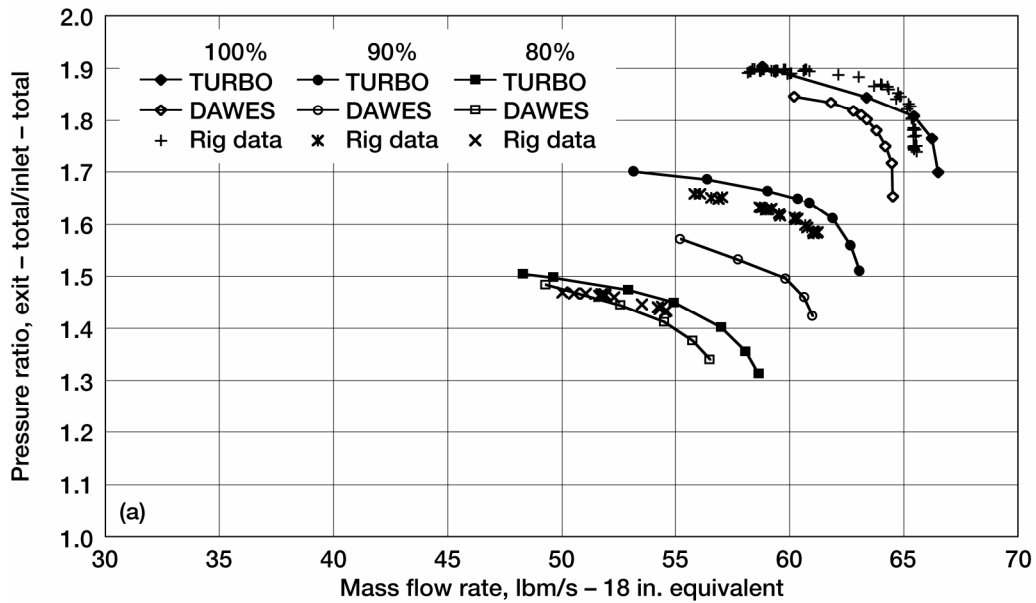


Figure 2.—(a) Pressure ratio variation calculated using TURBO code. QHSF, TURBO steady, 15444, 13900, and 12355 rpm. (b) Efficiency variation calculated using TURBO code. QHSF, TURBO steady, 15444, 13900, and 12355 rpm.

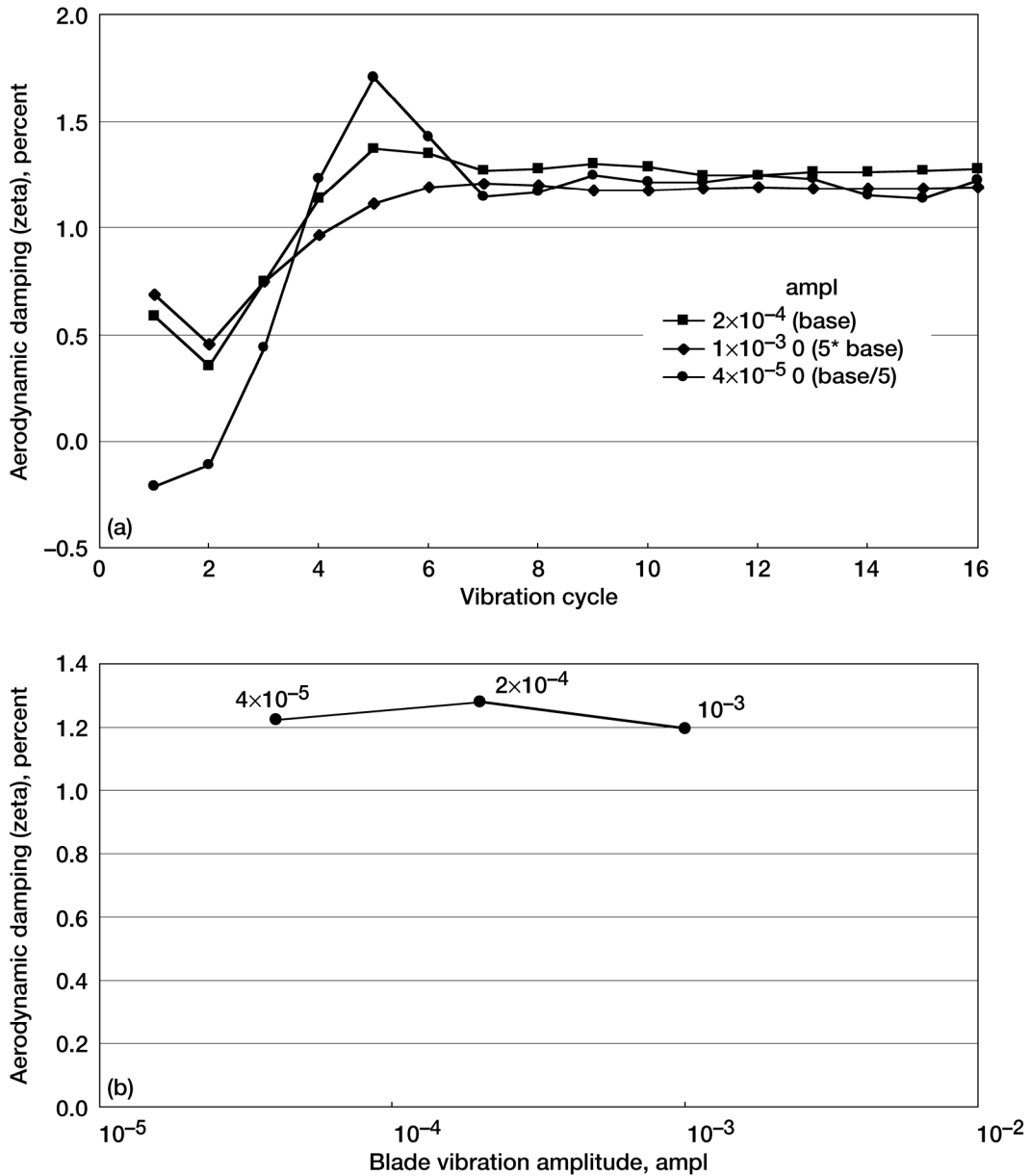


Figure 3.—(a) Convergence of unsteady TURBO solutions for different blade vibration amplitudes. Effect of vibration amplitude (ampl) base: ncyipc = 200, ampl = 2×10^{-4} , itend = 3, Cray C-90. (b) Variation of aerodynamic damping with blade vibration amplitude. Effect of vibration amplitude (ampl) base: ncyipc = 200, ampl = 2×10^{-4} , itend = 3, Cray C-90.

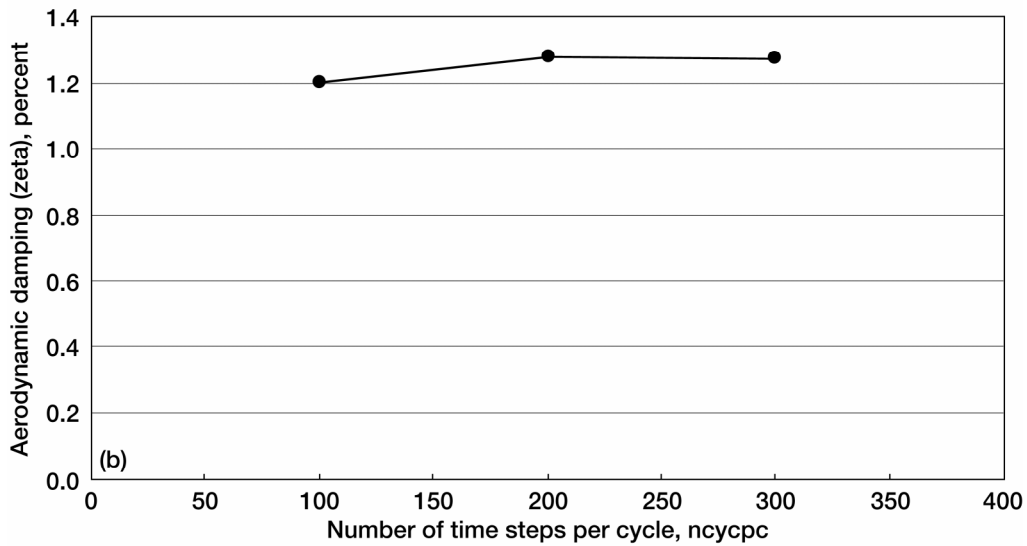
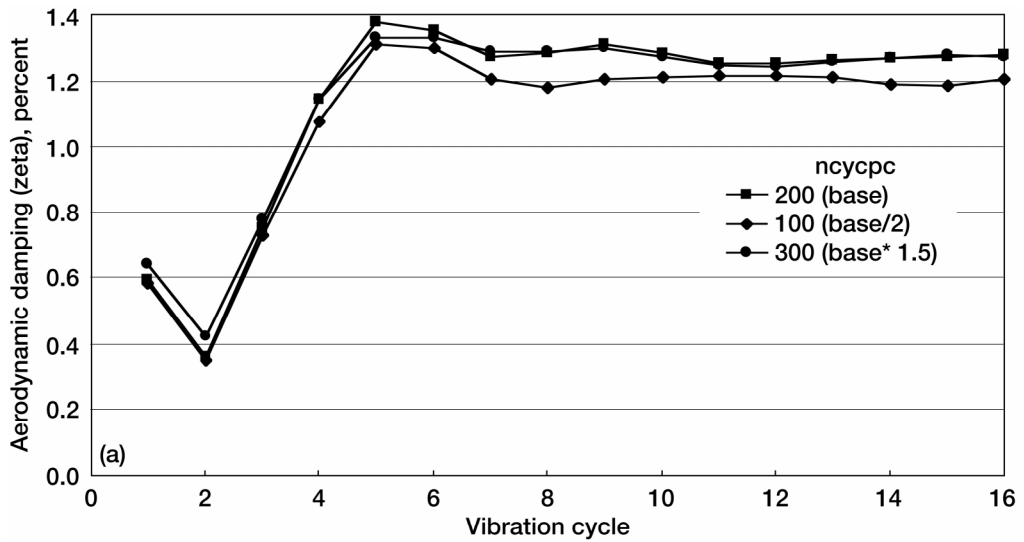


Figure 4.—(a) Convergence of unsteady TURBO solutions for different time steps. Effect of time steps per cycle (ncycpc) base: ncycpc = 200, ampl = 2×10^{-4} , itend = 3, Cray C-90. (b) Variation of aerodynamic damping with number of time steps per cycle. Effect of time steps per cycle (ncycpc) base: ncycpc = 200, ampl = 2×10^{-4} , itend = 3, Cray C-90.

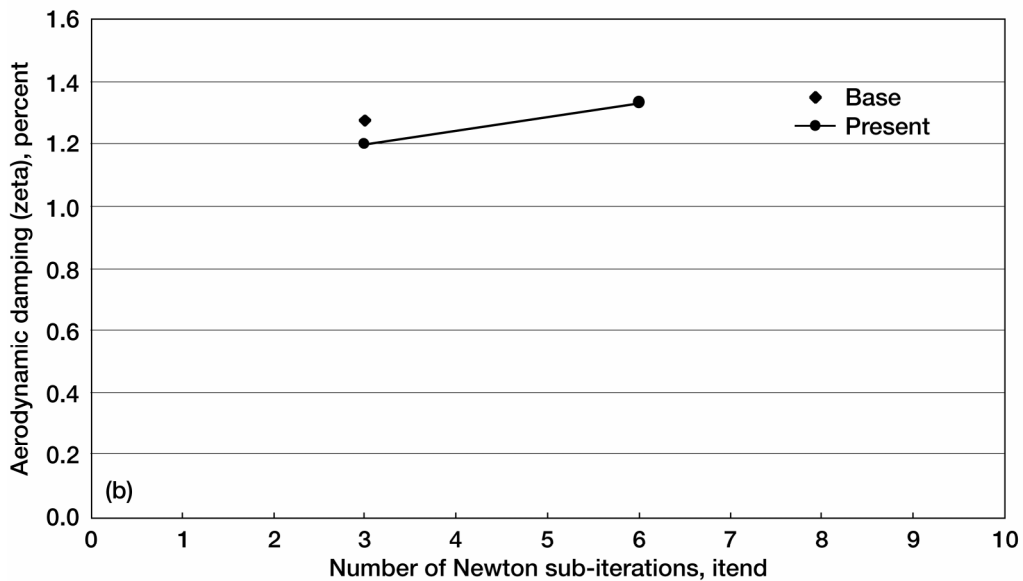
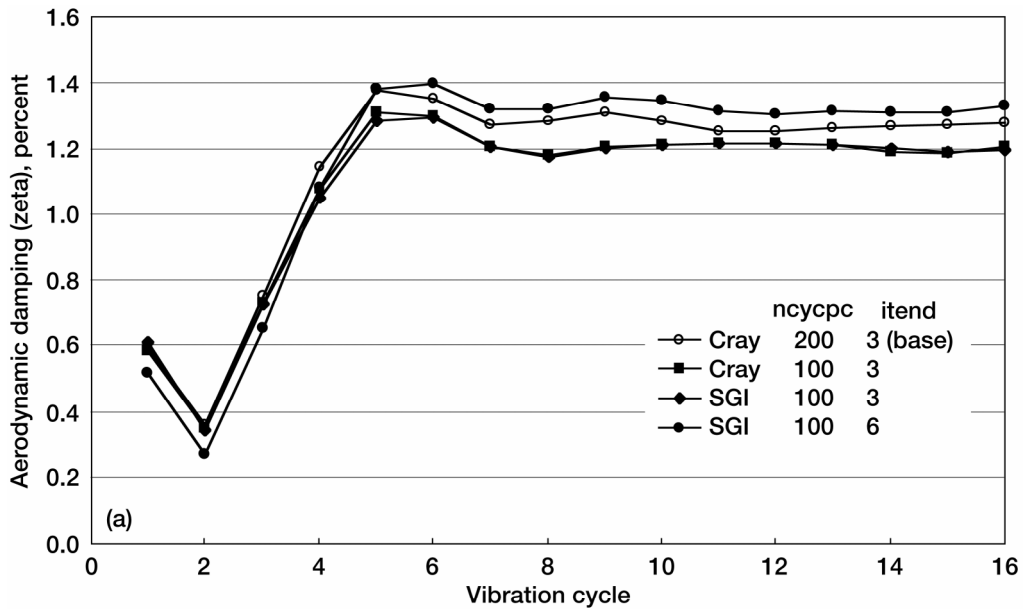
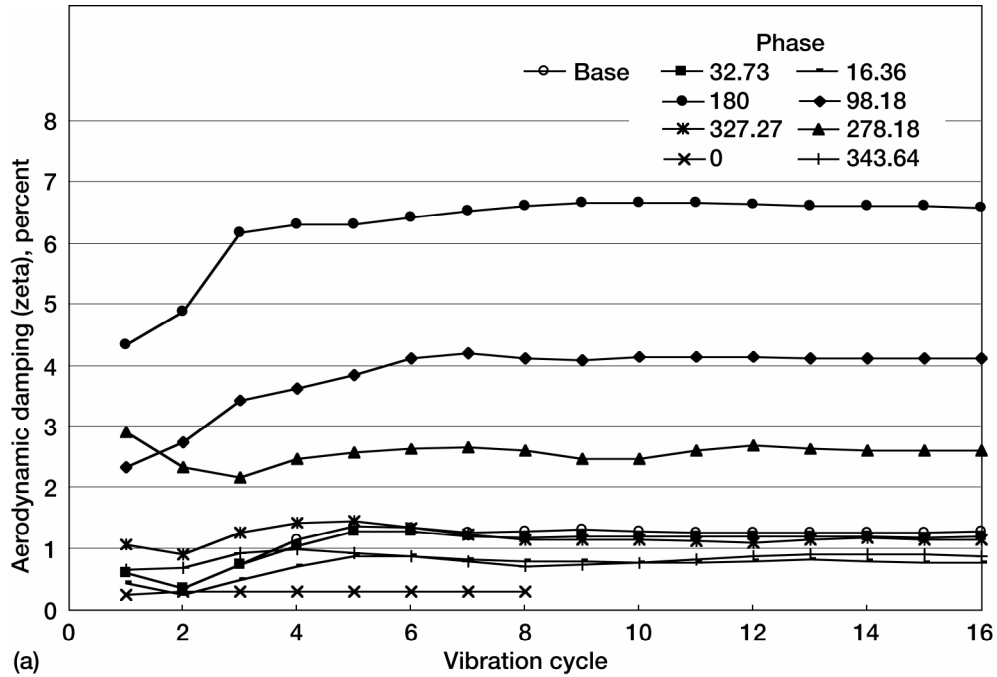
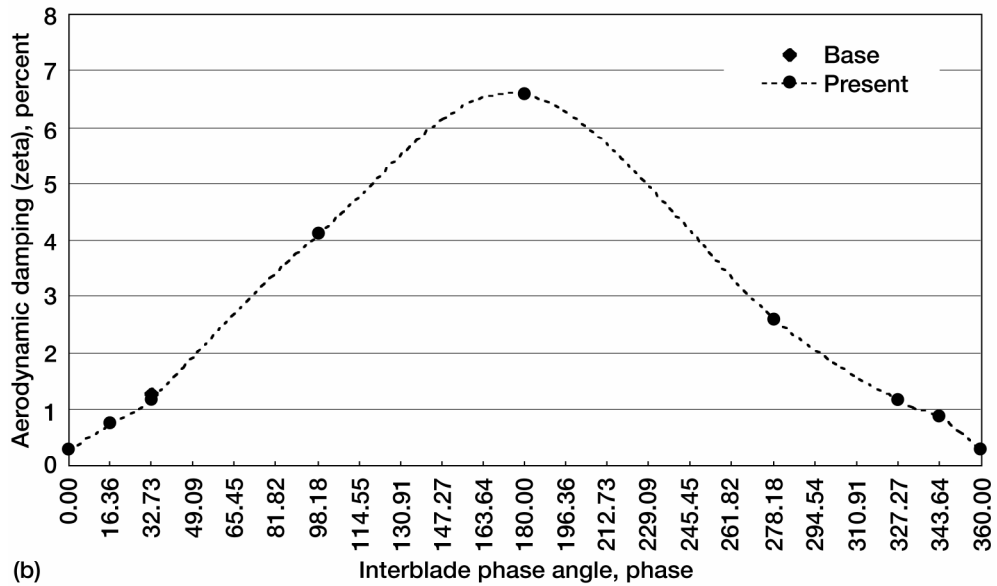


Figure 5.—(a) Convergence of unsteady TURBO solutions for different Newton sub-iteration counts. Effect of Newton sub-iterations (itend) base: ncyipc = 200, ampl = 2×10^{-4} , itend = 3, Cray C-90. (b) Variation of aerodynamic damping with maximum number of Newton sub-iterations. Effect of Newton sub-iterations (itend) base: ncyipc = 200, ampl = 2×10^{-4} , itend = 3, Cray C-90. Current: ncyipc = 100, ampl = 2×10^{-4} , SGI.



(a)



(b)

Figure 6.—(a) Convergence of unsteady TURBO solutions for different phase angles at 16 psi. Effect of interblade phase angle (phase) base: ncycpc = 200, ampl = 2×10^{-4} , itend = 3, Cray C-90, Phase = 32.73. Current: ncycpc = 100, ampl = 2×10^{-4} , itend = 3, SGI. (b) Variation of aerodynamic damping with interblade phase angle at 16 psi. Effect of interblade phase angle (phase) base: ncycpc = 200, ampl = 2×10^{-4} , itend = 3, Cray C-90, Phase = 32.73. Current: ncycpc = 100, ampl = 2×10^{-4} , itend = 3, SGI.

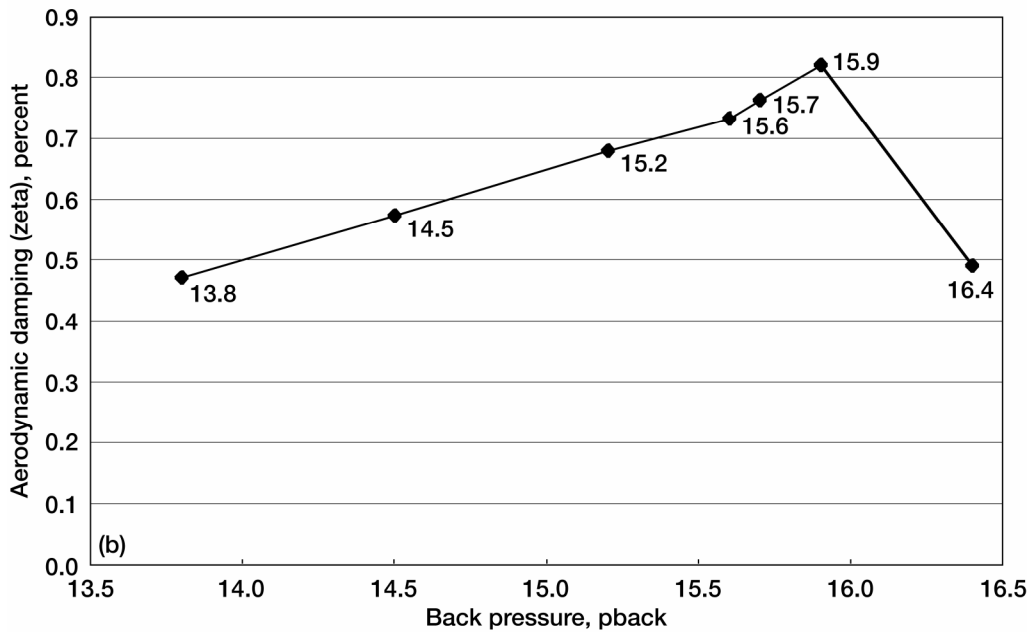
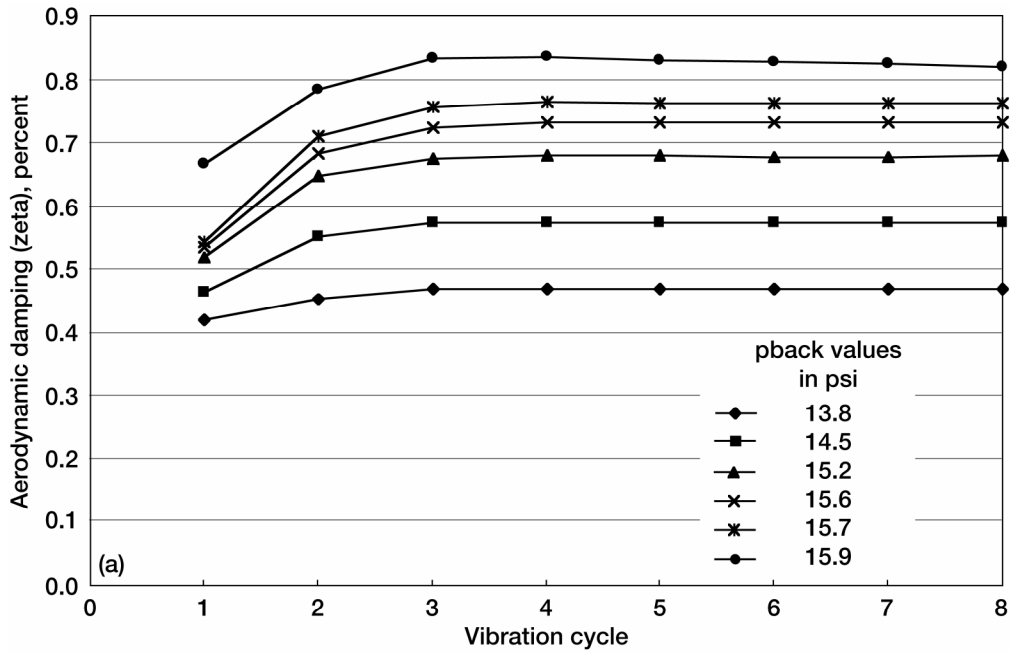


Figure 7.—(a) Convergence of unsteady TURBO solutions for different back pressures at 0° phase angle. 90 percent speed, phase = 0° (b) Variation of aerodynamic damping with back pressures at 0° phase angle. 90 percent speed, phase = 0° .

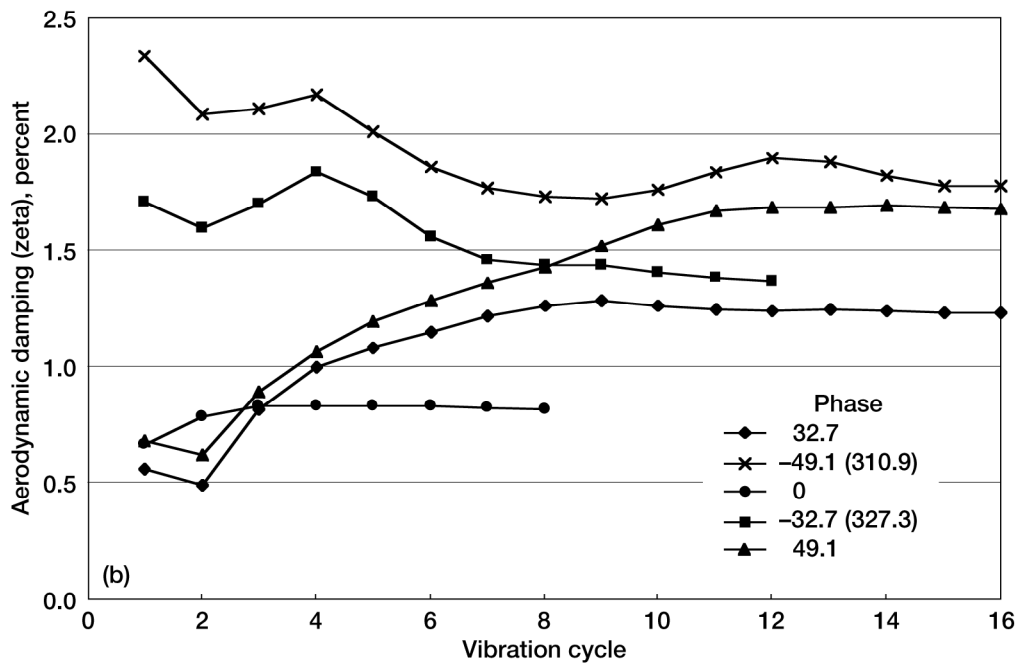
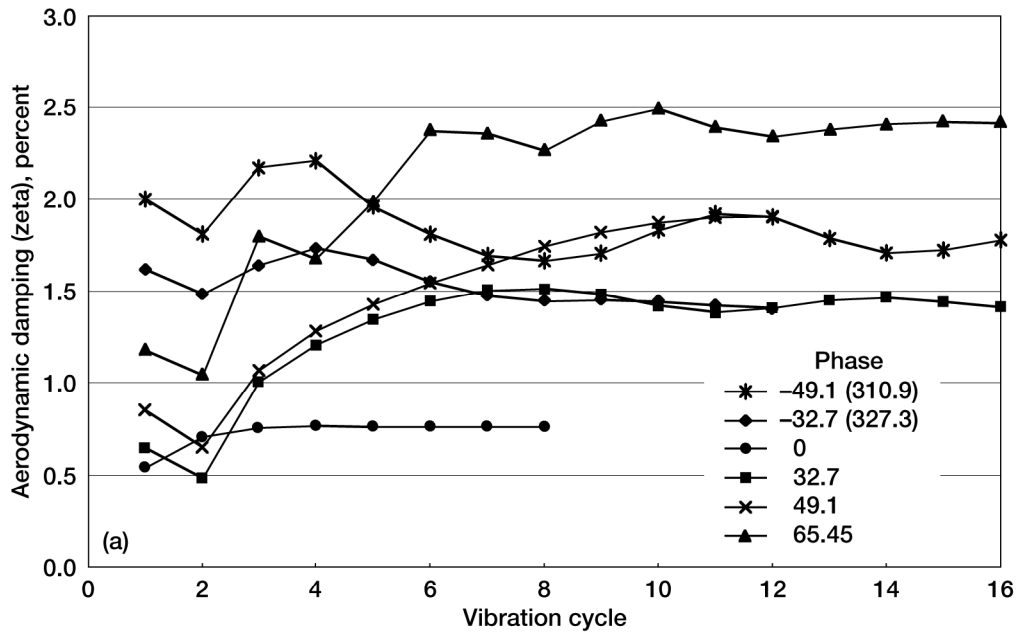


Figure 8.—(a) Convergence of unsteady TURBO solutions for different phase angles at 15.7 psi, 90 percent speed. (b) Convergence of unsteady TURBO solutions for different phase angles at 15.9 psi, 90 percent speed.

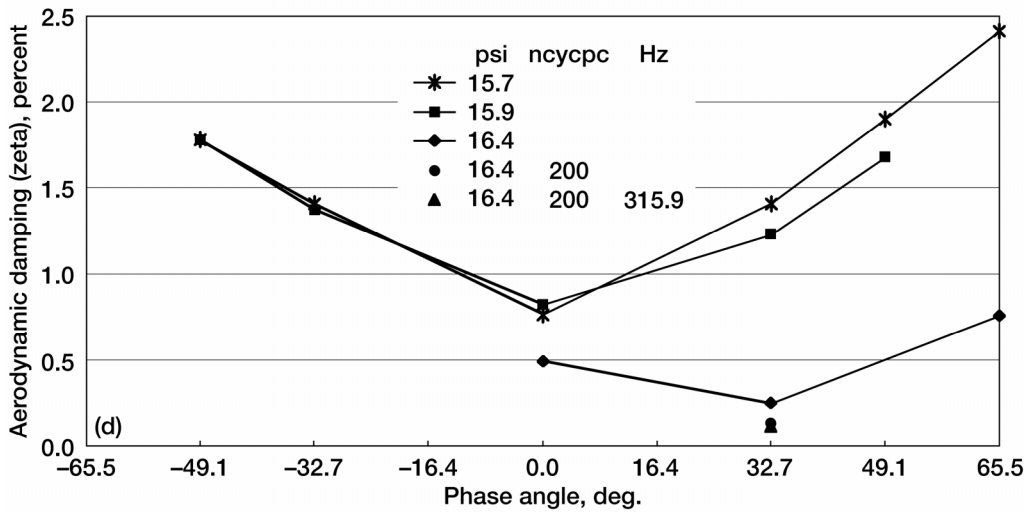
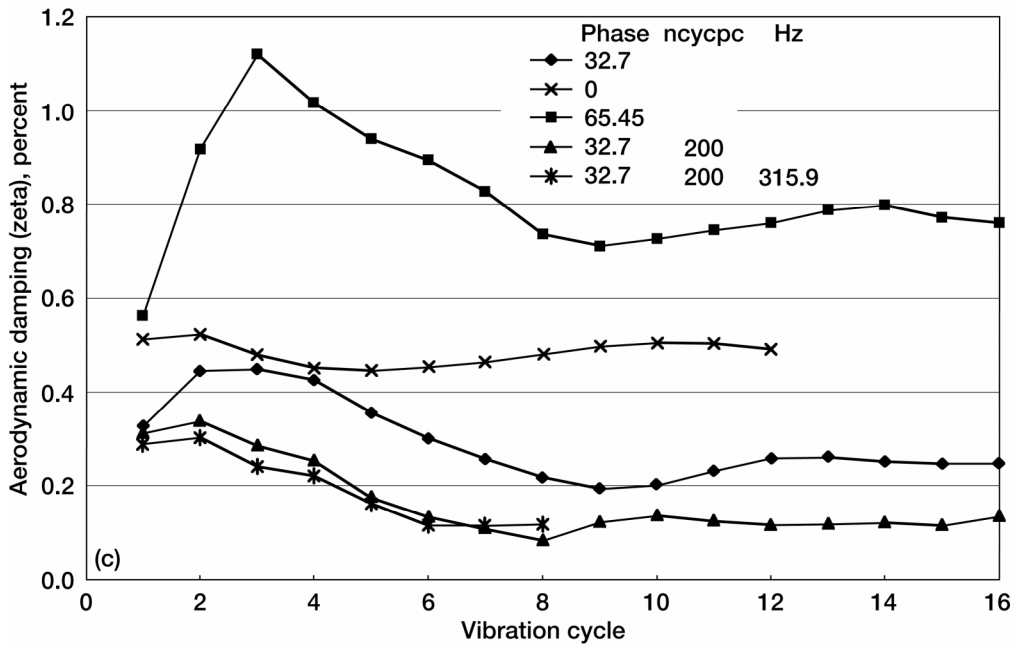


Figure 8.—(c) Convergence of unsteady TURBO solutions for different phase angles at 16.4 psi, 90 percent speed. (b) Variation of aerodynamic damping with back pressure, 90 percent speed.

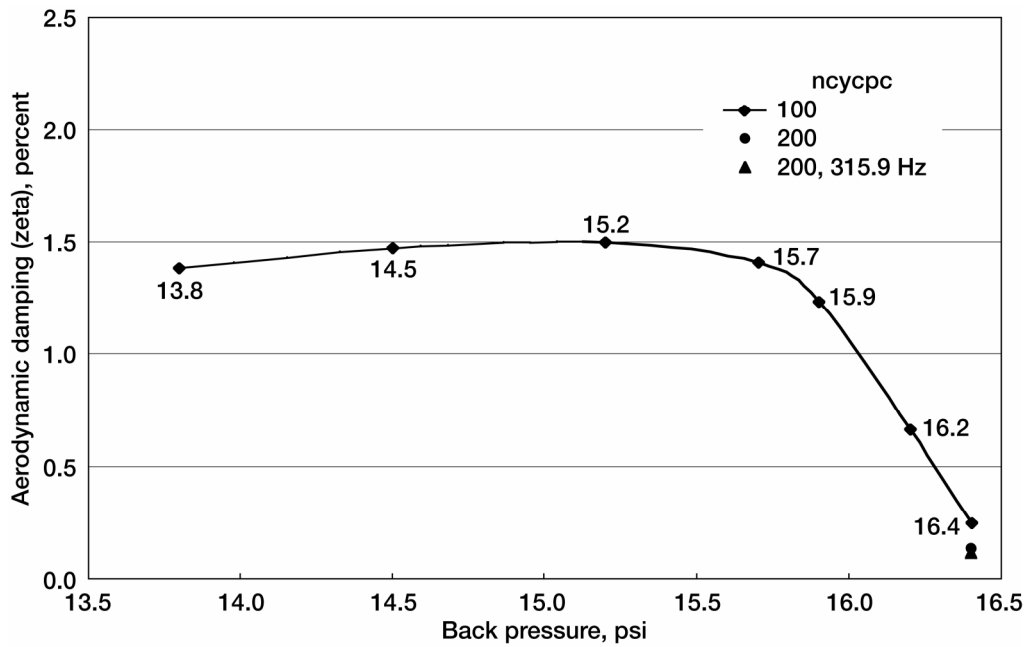


Figure 9.—Variation of aerodynamic damping with back pressure at 32.7° phase angle. 90 percent speed, 32.7° phase.

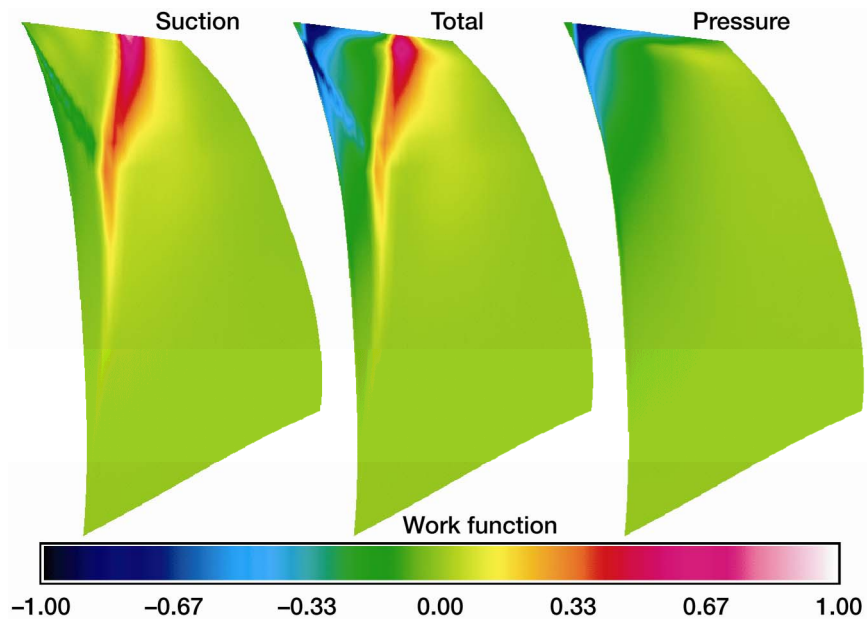


Figure 10.—Distribution of work-per-cycle on the blade surfaces for 90 percent speed, 16.4 psi back pressure, and 32.7° phase angle.

REPORT DOCUMENTATION PAGE			<i>Form Approved</i> <i>OMB No. 0704-0188</i>	
Public reporting burden for this collection of information is estimated to average 1 hour per response, including the time for reviewing instructions, searching existing data sources, gathering and maintaining the data needed, and completing and reviewing the collection of information. Send comments regarding this burden estimate or any other aspect of this collection of information, including suggestions for reducing this burden, to Washington Headquarters Services, Directorate for Information Operations and Reports, 1215 Jefferson Davis Highway, Suite 1204, Arlington, VA 22202-4302, and to the Office of Management and Budget, Paperwork Reduction Project (0704-0188), Washington, DC 20503.				
1. AGENCY USE ONLY (Leave blank)		2. REPORT DATE September 2006	3. REPORT TYPE AND DATES COVERED Technical Memorandum	
4. TITLE AND SUBTITLE Quiet High Speed Fan (QHSF) Flutter Calculations Using the TURBO Code			5. FUNDING NUMBERS WBS 984754.02.07.03.05.01	
6. AUTHOR(S) Milind A. Bakhle, Rakesh Srivastava, Theo G. Keith, Jr., James B. Min, and Oral Mehmed				
7. PERFORMING ORGANIZATION NAME(S) AND ADDRESS(ES) National Aeronautics and Space Administration John H. Glenn Research Center at Lewis Field Cleveland, Ohio 44135-3191			8. PERFORMING ORGANIZATION REPORT NUMBER E-15656	
9. SPONSORING/MONITORING AGENCY NAME(S) AND ADDRESS(ES) National Aeronautics and Space Administration Washington, DC 20546-0001			10. SPONSORING/MONITORING AGENCY REPORT NUMBER NASA TM-2006-214375	
11. SUPPLEMENTARY NOTES This report was originally published internally as QAT-001 in September 2002. Milind A. Bakhle, currently with NASA Glenn Research Center; Rakesh Srivastava currently with Honeywell, Engines, Systems, and Services, 111 S. 34th Street, Phoenix, Arizona; Theo G. Keith (Retired); James B. Min and Oral Mehmed (Retired), NASA Glenn Research Center. Responsible person, Milind A. Bakhle, organization code RXS, 216-433-6037.				
12a. DISTRIBUTION/AVAILABILITY STATEMENT Unclassified - Unlimited Subject Category: 07 Available electronically at http://gltrs.grc.nasa.gov This publication is available from the NASA Center for AeroSpace Information, 301-621-0390.			12b. DISTRIBUTION CODE	
13. ABSTRACT (Maximum 200 words) A scale model of the NASA/Honeywell Engines Quiet High Speed Fan (QHSF) encountered flutter wind tunnel testing. This report documents aeroelastic calculations done for the QHSF scale model using the blade vibration capability of the TURBO code. Calculations at design speed were used to quantify the effect of numerical parameters on the aerodynamic damping predictions. This numerical study allowed the selection of appropriate values of these parameters, and also allowed an assessment of the variability in the calculated aerodynamic damping. Calculations were also done at 90 percent of design speed. The predicted trends in aerodynamic damping corresponded to those observed during testing.				
14. SUBJECT TERMS Aeroelasticity; Flutter; Turbofan; Navier-Stokes; Unsteady flow			15. NUMBER OF PAGES 21	
			16. PRICE CODE	
17. SECURITY CLASSIFICATION OF REPORT Unclassified	18. SECURITY CLASSIFICATION OF THIS PAGE Unclassified	19. SECURITY CLASSIFICATION OF ABSTRACT Unclassified	20. LIMITATION OF ABSTRACT	

